Friedrich-Schiller-Universität Jena

Faculty of Biological Sciences

Max-Planck-Institute for Chemical Ecology

Department for Evolutionary Neuroethology
Project Group for Lepidopteran Neuroethology

"Mapping of odor-induced neuronal activity in the insect brain using immunohistochemistry"

Bachelor thesis

to obtain the degree of a

Bachelor of Science Biology

presented by

Luka Hecht

from Jena

Jena, 29.09.2021

Reviewers:

Dr. Sonja Bisch-Knaden

Prof. Dr. Nicole van Dam

List of content

Summary ..... **I**

Zusammenfassung ..... **II**

I. List of figures ..... **IV**

II. List of tables ..... **V**

III. List of abbreviations ..... **VI**

Introduction **1**

Model organism Manduca sexta *2*

Olfactory processing in Manduca sexta *2*

Aim of the project *6*

Material **7**

1. Chemicals *7*

2. Buffer, media, solutions and antibodies *7*

3. List of instruments and software *8*

Methods **10**

1. Insect rearing *10*

2. Anterograde tracing of the glomerulus *10*

3. Odor stimulation *11*

4. Immunohistochemical detection of activated glomeruli using anti-pERK antibody *12*

5. Data analysis *13*

Significance tests *14*

Results **15**

1. Optimized resolution through Alexa fluor 405 ..... *15*

2. Relative brightness in different stacks is brighter under HEB *17*

3. Significant differences in stack 1 and 8 through HEB *19*

4. Landmark glomeruli process HEB and GUA *20*

Landmark glomeruli DM4 and PL5 process HEB *20*

Landmark glomeruli VL3 and V1 process GUA *21*

References **26**

Acknowledgement **29**

Declaration of Independent Assignment **30**

Summary

The sense of smell plays a key role in the discrimination and localization of biologically important odorants, without it neither reproduction nor the survival of individual species can be ensured. In addition, the homologous structure of the olfactory bulbs of vertebrates and the antennal lobes of insects allows conclusions to be drawn about general mechanisms for odor processing in the brain (Hildebrand and Shepherd 1997). In insects, olfactory information is first transported to the primary processing center, the antennal lobes, which consist of functional subunits, the olfactory glomeruli. These in turn process a wide range of odors.

We sought to establish an immunohistochemical method to track odor-induced neuronal activity in the antennal lobe of the tobacco hawkmoth *Manduca sexta*. Specifically, we wanted to know if we could identify all glomeruli involved in the detection of two odors known to activate different regions in the antennal lobe (Bisch-Knaden et al. 2018) using pERK, a marker for neural activity.

We started several experiments where we tried out three different antibodies against pERK, different incubation times, odor-exposure times, and the two odors *cis*-3-Hexenyl benzoate and 4-Ethylguaiacol.

The left antenna of an immobilized animal was exposed to an odorant, while the right antenna was cut immediately before the experiment. After odor-exposure, the brain of the animal was quickly dissected, and incubated with a primary antibody against pERK. Regions where pERK was bound were then visualized with a second, fluorescent antibody, and studied under the confocal microscope.

When we compared the relative brightness of glomeruli at the odor-exposed side with the relative brightness of the corresponding glomeruli at the control side, we found that two glomeruli were brighter, i.e., became activated by each of the two odors we tested. These two active glomeruli were different between the odors and fit to the results of the calcium imaging in previous studies (Bisch-Knaden, Dahake et al. 2018), suggesting that pERK may be useful for localizing activated glomeruli. However, the result was not directly visible under the confocal microscope as in previous studies and was time consuming.

Keywords: *Manduca sexta*, olfaction, 4-Ethylguaiacol, cis-3-Hexenyl benzoate, antennal lobes, landmark glomeruli

Zusammenfassung

Der Geruchssinn spielt eine Schlüsselrolle bei der Unterscheidung und Lokalisierung biologisch wichtiger Geruchsstoffe, ohne die weder die Fortpflanzung noch das Überleben einzelner Arten gesichert werden kann. Darüber hinaus lässt der homologe Aufbau der Riechkolben von Wirbeltieren und den Antennenlappen von Insekten Rückschlüsse auf allgemeine Mechanismen der Geruchsverarbeitung im Gehirn zu (Hildebrand und Shepherd 1997). Bei Insekten wird die Geruchsinformation zunächst zum primären Verarbeitungszentrum, den Antennallappen, transportiert, die aus funktionellen Untereinheiten, den Glomeruli, bestehen. Diese wiederum verarbeiten eine breite Palette von Gerüchen.

Wir wollten eine immunhistochemische Methode entwickeln, um die geruchsinduzierte neuronale Aktivität im Antennallappen des Tabakschwärmers *Manduca sexta* zu verfolgen. Konkret wollten wir wissen, ob wir alle Glomeruli identifizieren können, die an der Erkennung von zwei Gerüchen beteiligt sind, von denen bekannt ist, dass sie unterschiedliche Regionen im Antennallappen aktivieren (Bisch-Knaden et al. 2018), indem wir pERK, einen Marker für neuronale Aktivität (Mirich, Illig et al. 2004), verwenden.

Wir starteten mehrere Experimente, in denen wir drei verschiedene Antikörper gegen pERK, unterschiedliche Inkubationszeiten, Geruchsexpositionszeiten und die beiden Geruchsstoffe *cis*-3-Hexenylbenzoat und 4-Ethylguaiacol ausprobierten. Die zweite Antikörperfärbung gegen pERK sollte helfen, die aktivierten Glomeruli zu identifizieren, die den jeweiligen Geruch verarbeiten.

Die linke Antenne eines immobilisierten Tieres wurde einem Geruchsstoff ausgesetzt, während die rechte Antenne unmittelbar vor dem Experiment abgeschnitten wurde. Nach der Geruchsexposition wurde das Gehirn des Tieres schnellstmöglich seziert und mit einem primären Antikörper gegen pERK inkubiert. Die Bereiche, in denen pERK gebunden war, wurden dann mit einem zweiten, fluoreszierenden Antikörper sichtbar gemacht und unter dem Konfokalmikroskop untersucht.

Als wir die relative Helligkeit der Glomeruli auf der geruchsexponierten Seite mit der relativen Helligkeit der entsprechenden Glomeruli auf der Kontrollseite verglichen, stellten wir fest, dass zwei Glomeruli heller waren, d. h. durch jeden der beiden getesteten Gerüche aktiviert wurden. Die aktiven Glomeruli unterschieden sich zwischen den Gerüchen und stimmten mit den Ergebnissen der Kalzium-Bildgebung aus früheren Studien überein (Bisch-Knaden, Dahake et al. 2018), was darauf

hindeutet, dass pERK für die Lokalisierung von aktivierten Glomeruli geeignet sein könnte. Das Ergebnis war jedoch nicht wie in vorrausgegangenen Studien, direkt unter dem konfokalen Mikroskop sichtbar und erwies sich daher als zeitaufwändig.

I. List of figures

Figure	Page
1. Olfactory sensory organs of *Manduca sexta.*	**3**
2. Arrangement in the head of *Manduca sexta*	**4**
3. AL reconstruction of female *Manduca sexta*	**5**
4. Chemical structure depiction	**6**
5. Odor stimulation cartridge	**11**
6. Fixation of *M. sexta* for odor stimulation	**11**
7. Double immunofluorescence staining of *M. sexta* whole brain	**15**
8. pERK staining with different fluorescent antibodies	**16**
9. Brightness of eight stacks in the antennal lobe after stimulation with HEB	**17**
10. Brightness of eight stacks in the antennal lobe after stimulation with GUA	**18**
11. Comparison of the relative brightness in different stacks stimulated with HEB or GUA.	**19**
12. With HEB stimulated landmark glomeruli percentage difference in relative brightness against the respective landmark glomeruli on the control	**20**
13. With GUA stimulated landmark glomeruli percentage difference in relative brightness against the respective landmark glomeruli on the control	**21**

II. List of tables

Table	Page
Chemicals	**7**
Buffers, media, solutions, and antibodies	**7**
Instruments and software	**8**
Overview of the used odors and antibodies	**13**

III. List of abbreviations

AL	Antennal lobe
AN	Antennal nerve
GUA	4-Ethylguaiacol
Gl	Glomerulus
HEB	*cis*-3-Hexenyl benzoate
M. sexta	*Manduca sexta*
MGC	Macroglomerular complex
OR	Odorant receptor
OSN	Olfactory sensory neuron
PBST	Phosphate-buffered saline
pERK	Phosphorylated extracellular signal-regulated kinase
SEG	Suboesophageal ganglion

Introduction

The sense of smell is of great importance to successfully discriminate and locate biologically important scents, such as those emitted to open up ecological niches, reproduce successfully or, above all, to enable survival (Riffell, Shlizerman et al. 2014). Olfactory cues enable animals to find suitable sexual partners, nesting sites, food and to avoid enemies (Couty, Van Emden et al. 2006, Hansson and Stensmyr 2011). Studying the interactions between the animals and their environment is essential to clarify ecological issues. Despite the major morphological differences between noses and antenna, vertebrate olfactory bulbs are functionally homologous to the insect AL because process odor molecules by the same mechanism. For this reason, insects are useful model organisms to understand the basics of information processing in the brain (Hildebrand and Shepherd 1997). The highly derived olfactory system in Lepidoptera, makes them to a perfect model organism for studying the olfactory system.

In particular, the tobacco hawkmoth *Manduca sexta* exhibits a high degree of ecologically relevant olfactory behavior that is adapted to its environment and its relationship with its host plants. For this reason, *M. sexta* has become a well-studied model organism in the field of olfaction in lepidopterans (Hildebrand 1995, Shields and Hildebrand 1999).

To identify the glomeruli, which are important for olfactory processing through the engram cells, confocal microscopes are used, which makes it possible to stain certain structures with fluorophores to detect even chemical processes in biological structures. To identify the engram cells, the increase in phosphorylated ERK (pERK) produced during the processing of a scent is determined by antibody staining (Miyashita, Kikuchi et al. 2018).

To date, numerous studies have been conducted on olfactory processing. But in *Manduca sexta*, the glomeruli of the AL on the the odor-processing side have not yet been visualized by pERK activation, as was the case in the blowfly *Phormia regina* or zebrafish (Yabuki, Koide et al. 2016, Maeda, Nisimura et al. 2020).

Model organism *Manduca sexta*

Studies on the tobacco hawkmoth *M. sexta*, a nocturnal insect of the family Sphingidae, have contributed versatile information regarding e.g. the larval growth stages (Rountree and Bollenbacher 1986), their genome (Kanost, Arrese et al. 2016), odor-induced activation patterns in the AL, odor-induced behavior (Bisch-Knaden, Dahake et al. 2018) and a lot more. Belonging to the large group of agricultural pests in the order of Lepidoptera, *M. sexta* caterpillars feed on solanaceous plants (e.g., tobacco and tomato). It is a typical holometabolous insect with five larval instars and is easy to rear under laboratory conditions. Larvae can be kept on artificial diet, grow to a weight of over 10 g and can reach a total size of 12 cm before pupation. The development takes only 50 to 55 days from the egg to the adult moth.
For the mating act the females release a pheromone blend with bombykal as the main component. This pheromone blend enables males to locate receptive females (Tumlinson, Brennan et al. 1989). For mated females, olfactory information is very important to find good oviposition sites where the fertilized eggs can develop properly (Reisenman and Riffell 2015), and to find nectar as well.

Olfactory processing in *Manduca sexta*

Moths are one of the most important insect models when it comes to olfaction due to their specific and sensitive sense of smell and their complex chemosensory behavior (Hansson 1995). Their parallel olfactory systems, for processing sex pheromones and CO_2, have been well characterized in recent years. The basic structure of the olfactory system of insects always follows the same schema. The neuronal processing of olfactory information first involves the receptor neurons in the sensilla, primary computations take place in the ALs, and further processing in the higher brain centers such as the mushroom bodies or the lateral protocerebrum (Galizia and Rössler 2010).

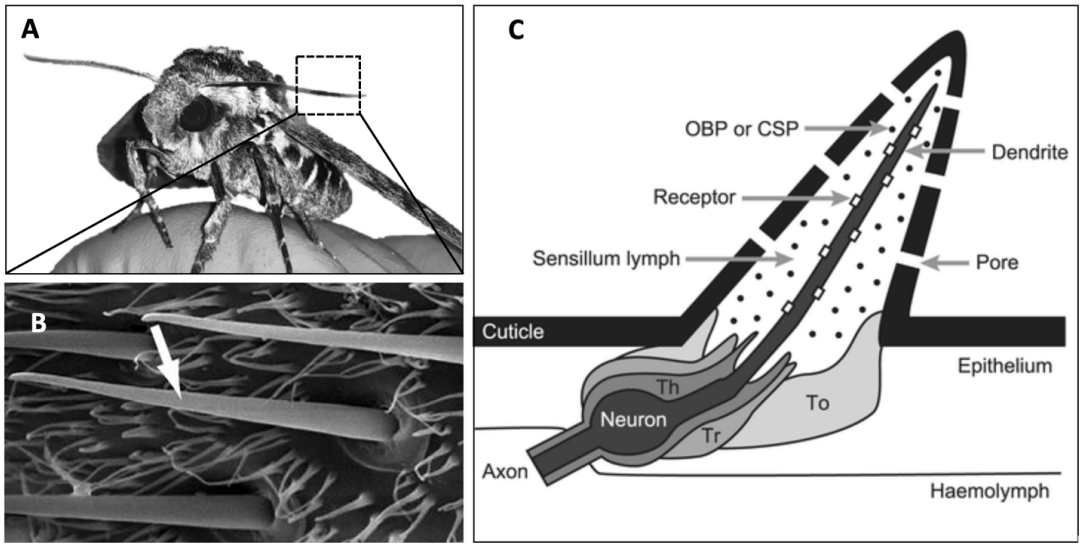

Figure 1: Olfactory sensory organs of Manduca sexta*. (A) Adult female tobacco hornworm with its antenna. (B) Antenna fine structure shown with an* scanning electron microscope image *(Ma, Zhao et al. 2017). Arrow points to an olfactory sensillum. (C) General schematic representation structure of a lepidopteran olfactory sensillum (Mitaka, Kobayashi et al. 2016). The cell body of the receptor neuron lies in the center, surrounded by the three accessory cells (thecogene, trichogen, tormogen). The outer dendritic segment is surrounded by sensillum lymph and can detect the chemicals through chemoreceptors. The signal is transmitted via the axon of the receptor neuron to the central nervous system, i.e., the antennal lobe (Hansson 1995)*

The antenna is the main olfactory organ of insects (Fig. 1A) and is densely covered with olfactory sensilla (Fig. 2B), which house olfactory sensory neurons (OSNs) whose dendritic part expresses the chemosensory receptors that bind odor molecules. To reach the receptors, the odorants diffuse through the cuticular pores into the sensillum lymph, guided by olfactory binding proteins (OBPs) (Figure 1C). For the detection of these short-lived chemicals, there are two different types of receptors, the ionotropic receptors (IRs) and the olfactory receptors (ORs). The ORs form the largest species-specific group of chemoreceptors, which forms about 72 in *M. sexta* (Grosse-Wilde, Kuebler et al. 2011). After binding of an odor molecule to an OR, the respective OSN transmits the information to the brain. The first olfactory processing center is the AL, where OSNs expressing the same OR converge to the same olfactory glomerulus (Hansson 1995, Mitaka, Kobayashi et al. 2016).

In nature, insects always perceive pheromones in a with scents filled environment released by plants, animals and so on. However, out of these surroundings only a few chemicals do have a value for the insect's ecology. The olfactory system of the males has evolved a strategy to detect low concentrated sex pheromones released by females. This adaption involves an increased surface area of the antenna, and affects the peripheral pheromone-detecting system, called the macroglomerular complex (MGC) found in male M. sexta to locate mates (Galizia and Rössler 2010). A multiplier effect

is achieved by additional increase detecting neurons and a higher sensitivity of the individual detectors.

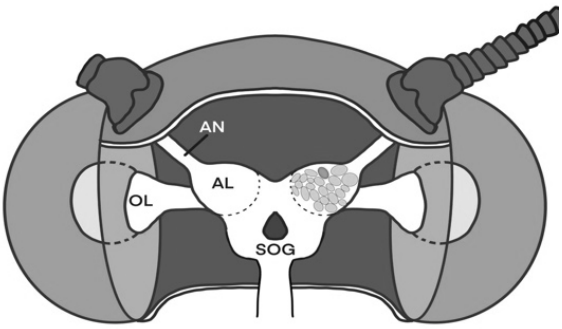

Figure 2: Arrangement in the head of Manduca sexta (frontal). *Detailed view of the different brain regions of M. sexta, (after removing the scales, cuticle, fat tissue etc.) including the antennal nerves (ANs), suboesophageal ganglion (SOG), optic lobes (OLs), and the antennal lobes (ALs) with the olfactory glomeruli. The airstream was directed to the left antenna, while the right antenna was disconnected by microscissors.*

These adaptations at the level of the antenna are also reflected in the antennal lobe. The AL is a conglomerate of anatomically distinct subunits of glomeruli. All OSNs expressing the same receptor converge to the same glomerulus (Vosshall, Wong et al. 2000). An obvious division within the male AL is the separation between enlarged, pheromone-specific glomeruli, termed the MGC, and a set of general glomeruli. The MGC serves as an example of how strong selection pressure, in this case to increase sensitivity to sex pheromones in male *M. sexta*, can lead to pronounced size differences between olfactory glomeruli.

Female *M. sexta* also exhibit two such enlarged glomeruli at a similar position as the MGC in males, so-called large female glomeruli (LFGs). These LFGs might be involved in female-specific behaviors such as searching for suitable oviposition sites (King, Christensen et al. 2000).

Males devote themselves to finding females and nectar, while females search for suitable egg-laying sites in addition to nectar sources. These different requirements led to the evolution of a sexually dimorphic olfactory system in moths (Bisch-Knaden, Dahake et al. 2018).

In their natural habitat the diffusion of scents, a mixture of chemical constituents, trigger different responses from central neurons in the brain. Because of this diversity of natural odorants, it is difficult to identify patterns of neuronal activity and resulting behavioral responses. This is particularly difficult in the early stages of processing, such as in ALs, because different neural codes can play overlapping roles (Riffell, Lei et al. 2009).

So far, only for the lateral LFG it is known which odors are processed by this glomerulus (King et al. 2000). All other glomeruli in the female AL still have to be

deorphanized, i.e., the activating odors have to be identified. We know from *in vivo* calcium imaging studies with *M. sexta* that each odor evokes an odor-specific activation pattern across the AL (Bisch-Knaden et al. 2018). However, as the boundaries of glomeruli are not visible in these experiments, and as the glomeruli's shape and position might be very different *in vivo* and *in vitro* (Grabe et al. 2015), an assignment of *in vivo* activation patterns to an *in vitro* reconstruction of AL glomeruli is not possible (Figure 3). In addition, calcium imaging experiments are restricted to the most dorsal layer of glomeruli, leaving half of the glomeruli on the ventral side of the AL unexplored.

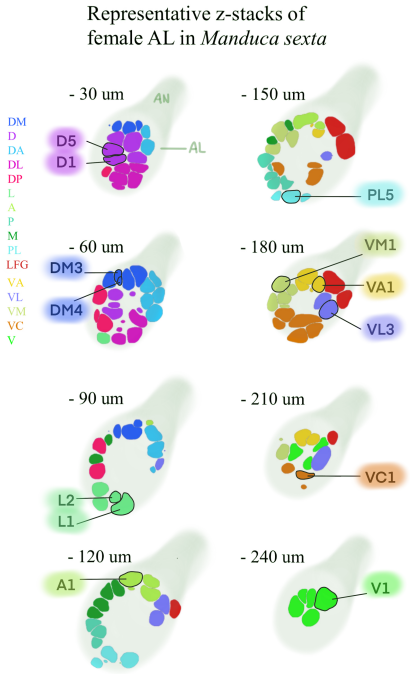

Glomeruli group	Landmark glomeruli	Internal array
Dorsal (D)	D1, D5	D1, D2, D3, D4, D5
Dorsal-Anterior (DA)	-	DA1, DA2, DA3, DA4, DA5
Dorsal-Posterior (DP)	-	DP1, DP2, DP3
Dorsal-Lateral (DL)	-	DL1, DL2, DL3, DL4, DL5
Dorsal-Medial (DM)	DM3, DM4	DM1, DM2, DM3, DM4, DM5, DM6
Lateral (L)	L1, L2	L1, L2, L3, L4
Anterior (A)	A1	A1, A2, A3, A4
Medial (M)	-	M1, M2, M3, M4
Posterior (P)	-	P1, P2, P3, P4, P5
Posterior-Lateral (PL)	PL5	PL1, PL2, PL3, PL4, PL5
Ventral-Anterior (VA)	VA1	VA1, VA2, VA3, VA4
Ventral-Lateral (VL)	VL3	VL1, VL2, VL3, VL4
Ventral-Medial (VM)	VM1	VM1, VM2, VM3, VM4, (VM5)
Ventral-Center (VC)	VC1	VC1, VC2, VC3, VC4
Ventral (V)	V1	V1, V2, V3, V4, V5

Figure 3: Reconstruction of the left AL in 8 stacks of female Manduca sexta*. (Yusuke Shiota, unpublished)*

A promising new method to trace odor-induced neural activity to the AL using immunohistochemistry was described in blowfly and zebrafish (Yabuki, Koide et al. 2016, Maeda, Nisimura et al. 2020).

Differential staining in glomerular regions was demonstrated by anterograde fluorescent labeling of the afferent nerves of the antenna. In glomeruli activated by natural odorants, second antibody staining of phosphorylated extracellular signal-regulated kinase (pERK) occurred. Different odorants (Figure 4) should activate different glomeruli of the standard map (Figure 3). To better distinguish the stimulated regions, two odorants processed in different regions of the AL were chosen, HEB (closer to the AL entrance) and GUA (closer to the ventral-lateral side)(Bisch-Knaden,

Dahake et al. 2018). These were administered under different conditions. The resulting signal was then fixed and visualized by immunostaining under the confocal microscope.

A

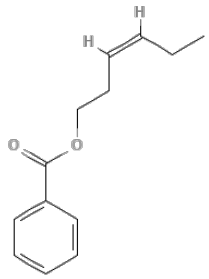

B

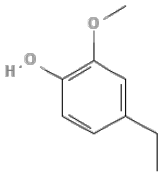

Figure 4: Chemical structure depiction *of (A) (Biotechnology HEB 2021) cis-3-Hexenyl benzoate and (B) (Biotechnology GUA 2021) 4-Ethylguaiacol.*

Among the approximately 70 glomeruli, there are some that are often in the same position and have a characteristic shape. Thus, they help to divide the brain into 8 stacks (30 µm apart from each other) that can be identified in each animal. These glomeruli are so-called landmark glomeruli, and belong to subgroups, which were named based on their location (Figure 3; Yusuke Shiota, unpublished), similar to the nomenclature used in former studies with the vinegar fly, *Drosophila melanogaster* (Couto, Alenius et al. 2005, Grabe, Baschwitz et al. 2016).

Aim of the project

In this study, we tried to establish an immunohistochemical method to trace odor-induced neural activity in the AL of *M. sexta*. Specifically, we wanted to know if we could identify all glomeruli involved in the detection of each of two odors using immunostaining with pERK.

Material

1. Chemicals

Chemical	Formula	Company
Cis-3-Hexenylbenzoate (HEB)	C6H5CO2CH2CH2CH =CHC2H5	MerckKGaA: SIGMA-ALDRICH, St. Louis, USA, Art. No. W368806
4-Ethylguaiacol (GUA)	C2H5C6H3-2-(OCH3)OH	MerckKGaA: SIGMA-ALDRICH, St. Louis, USA, Art. No. W243604
Ethanol 99,8% denatured	C2H6O	Carl ROTH, Gmbh + Co. KG, Karlsruhe, Germany, Art. No. K928.3
Methyl salicylate	C6H4CO2CH3	MerckKGaA: SIGMA-ALDRICH, St. Louis, USA, Art. No. M6752
TritonX100		MerckKGaA: SIGMA-ALDRICH, St. Louis, USA, Art. No. T8532-500ML
Histo VT one		Innovations for life science Nacalai, USA Art. No. 06380

2. Buffer, media, solutions and antibodies

1M PBS (pH 7,4)		0,2M Na_2HPO_4 0,2M NaH_2PO_4 NaCl ddH_2O
1M PBST (0,2 % Triton)		49ml PBS 1ml 10% Triton X
Blocking solution 2 % NGS		50ml PBST
Fixation solution TCA		10% TCA
Ringer solution (*M. sexta*) (pH 6,9)		150 mM NaCl 3 mM CaCL2 3 mM KCl 10 mM TES buffer 25 mM Sucrose
Antibodies	Monoclonal	1st Antibody:

		Rabbit α-pERK (9106, Cell signaling) Mouse α-Syn ORF 2nd Antibody (Attenuation 1:300 in PBST with 1% NGS) Goat α-rabbit Alexa fluor 405 Goat α-mouse Alexa fluor 633
	Polyclonal	1st Antibody: Mouse α-pERK (9101, Cell signaling) 2nd Antibody: Goat α-mouse 568
Phos Stop pH 7.4		0,2M Na_2HPO_4 0,2M NaH_2PO_4 NaCl ddH_2O

3. List of instruments and software

Instrument /Software	**Model**	**Manufacturer**
Amira		
Dental wax	Erkogum transp.	Erkodent Erich Kopp GmbH Pflanzgrafenweiler, Germany
Confocal Microscope	LSM 880 VIS Microscope	Zeiss, Jena, Germany
Concave-Convex Jaws	Item. No. 10053-09	Fine Science Tools, Foster City, USA
Dumont Dumoxel Tweezers	14098 #5, 0.1 x 0.06 mm	World Precision Instruments Sarasota, USA
Dissecting scissors	14393	World Precision Instruments Sarasota, USA
ImageJ	ImageJ bundled with Zulu OpenJDK 13.0.6	Research Services Branch
Insect pins	Original EmilArltz Insect Pins, 1	Original EmilArltz, Austria
Logic Module	Siemens LOGO! 24 RCE - 6ED1052-1HB08-0BA1	Siemens AG, Nuremberg, Germany
Microcentrifuge	Sprout	Biozym Scientific GmbH Oldendorf, Germany
Microscope Cover Glasses	Menzel- Gläser, 22 x 22 mm	Carl Roth GmbH & Co. KG Karlsruhe, Germany
Microscope light	Olympus, KL200	SCHOTT AG Mainz, Germany
Modeling Clay	622 415	Pelikan

		Hannover, Germany
Object carrier folder	Nr. 51.850.042	CEESEM
Pasteur pipettes	Pasteur pipettes, without cotton stopper	Carl Roth GmbH & Co. KG Karlsruhe, Germany
Pipet	Gilson Pipetman	Gilson International Villiers le bel France
Pipet Tip	Tip One	STARLAB GmbH Hamburg, Germany
Precision Wipes	05511	Kimberley-Clark Europe Reigate, United Kingdom
Protective case	PELI 1120 Case	PELI Products, S.L.U. USA
Rocker-Shaker	Mini Rocker Shaker MR-1	Biosan SIA Latvia
Rotary Mixer	PELCO R2 Rotator	
Round Filters	Rotilabo type 601A	Carl Roth GmbH & Co. KG Karlsruhe, Germany
Stereomicroscope	Novex Stereomicroscope p-20	Euromex Microscopen bv Arnhem, Netherland
Stereomicroscope	Olympus Zoom-SZ51	
Thermomixer	Thermomixer compact 5350	Eppendorf AG (Hamburg, Germany)
Tissue	Rotizell	Carl Roth GmbH & Co. KG Karlsruhe, Germany
Vials	1.5 ml Vials N9 702283	Macherey-Nagel GmbH & Co. KG Düren, Germany
Glue	Pattex, Special glue, modeling plastic	Henkel AG & Co. Düsseldorf, Germany
Gloves	TouchNTuff	Ansell Brussels, Belgium
Tube for *M. sexta*		Workshop MPI, Jena, Germany
Vannas spring scissor	Item. No. 91501-09	Fine Science Tools, Foster City, USA
Vortex	Vortex-Genie 2 G-560E	Scientific Industries, New York, USA
Cotton	Ebelin cotton	dm Drogerie Market Karlsruhe, Germany
ZEN	ZEN 2.1 SP3	Zeiss International

Methods

1. Insect rearing

M. sexta were reared at the Max-Planck-Institute for Chemical Ecology, Jena, Germany. Some of the hatched animals were put into a flight cage for mating. For oviposition they had one of their hostplants, *Datura wrightii.* The eggs were collected and transferred to small boxes, which were kept inside a climate-controlled chamber at 50 % humidity and 24 to 26°C, and a light cycle of 9h dark and 15h light. The hatched caterpillars were also kept in boxes with an artificial diet (46 g agar, 144 g wheat germ, 140 g corn meal, 76 g soy flour, 75 g casein, 24 g salt mix, 36 g sugar, 5 g cholesterol, 12 g ascorbic acid, 6 g sorbic acid, 3 g methyl paraben, 9 ml linseed oil and 30 ml Vitamin mix (30 mg nicotinic acid, 15 mg riboflavin, 7 mg thiamine, 7 mg pyridoxine, 7 mg folic acid and 0.6 mg biotin per 1.8 ml water). Wandering fifth instar larvae were individually transferred into wooden boxes for pupation until one week before hatching. Then, the pupae were kept in egg cartons inside sex-separated climate chambers. Hatched animals were put into small paper bags inside the same climate-controlled chamber with a humidity of 60 to 70 % and 25°C. Moths were tested at day 1 to day 4 after emergence and had no experience with plant volatiles.

2. Anterograde tracing of the glomerulus

Adult female animals of 1-4 days after emergence were firmly restrained by putting in metal cones with the head exposed and immobilized by sealing with clay and cotton. That fore metal cones were specially produced by the workshop of the Max-Planck-Institute, Jena, Germany. For control the right antenna was cut by hand with vannas spring scissors at the antenna scape.

After the odor-treatment the brain was dissected by opening the capsule and removing labial palps, cibarial musculature and fat under a stereomicroscope while using Ringer's solution to prevent drying out and then fixed in 10 % Trichloroacetic acid (TCA) for 1h at room temperature. Moreover, putted into the first Antibody (92,5 % PBST, 4,9 % GSC, 1,6 % syn ORF/ 3H2 2D7, 1 % pERK) for one week at 4°C on a rocker-shaker. Afterwards the specimen was washed with 1M Phosphate Buffered Saline with 0,2 % Tween® 20 (PBST, pH 7.9) for 3 hours (4 x 15 min, 2 x 30 min, 1 x 1 h) it was stained in the second Antibody (α-Rabbit Alexa fluor 546, α-Mouse

Alexa fluor 466). After two days it was again washed in PBST for 3 hours and serially dehydrated with 50, 70, 80, 90, 96, 100 and 100 % ethanol for 15 min per solution; and then permeated with methyl salicylate. Further the specimens were observed under a confocal laser scanning microscope (LSM 880nVIS Microscope, Carl Zeiss) (Maeda, Nisimura et al. 2020).

3. Odor stimulation

The right antenna which was cut by vannas spring scissor at the antenna scalp serves as our negative control while the receptor axons of *M. sexta* just project to the spheroidal glomeruli in the ipsilateral antennal lobe (Christensen, Harrow et al. 1995). The left antenna on the other hand were exposed to a constant, moistened and charcoal-filtered air stream (compressed house air, 8 bar) regulated to a pressure of 5 bar, controlled by a logic module.

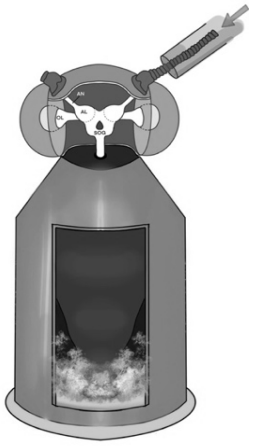

Figure 5: Fixation of *M. sexta* for odor stimulation. Airflow on the right antenna, cutted left antenna for control. Moth in a tube closed with cotton and clay.

Odor stimulation cartridges were prepared by dropping 10 µl of the mineral oil odors on 1 cm^2 filter paper circles, which were previously inserted into pasteur pipets and covered with a 1 ml pipette tip with blocking out material at the end to prevent evaporation (Figure 6).

The antenna gets pulled into an aluminum pipe (diameter 7 mm) with a hole 5 cm in front of the insect's antenna. Odor stimulations were archived by placing the end of each pasteur pipette into the small hole in the pipe and then letting a 10 min stream of humidified air run through the filter paper and into the air flow provided by the pipe (Figure 5).

***Figure 6: Odor stimulation cartridge**. Pasteur pipet filled with filter paper at the top a covered with two tips and blocking out material.*

In our experiments we used the ecologically relevant floral odorants *cis*-3-Hexenylbenzoate (HEB) and 4-Ethylguaiacol. The odors for the females were diluted in mineral oil and selected because of their ecological and physiological relevance as

shown in previous studies of *M. sexta.* Also these aromatic odors count as some of the most attractive odorants and had been shown through long proboscis contacts in tests (Shields and Hildebrand 2001, Bisch-Knaden, Dahake et al. 2018) and electrophysiological studies (King, Christensen et al. 2000).

4. Immunohistochemical detection of activated glomeruli using anti-pERK antibody

Anti-pERK antibody

The anti-pERK antibody specifically binds phosphorylated extracellular signal-regulated kinase (pERK) which is an required transcription factor for long-term memories (LTMs) (Miyashita, Kikuchi et al. 2018). First, we used the monoclonal antibody including Rabbit α-pERK (9106, Cell signaling) and Mouse α-Syn ORF as the first antibodies. For the second Antibody we tried two different Alexa fluor fluorescent proteins:

Goat α-rabbit Alexa fluor 488 and Goat α-mouse Alexa fluor 546

Goat α-rabbit Alexa fluor 405 and Goat α-mouse Alexa fluor 633

This antibodies were previously used in studies of zebrafish (Yabuki, Koide et al. 2016) and blowflies (Maeda, Nisimura et al. 2020).

Furthermore, we also tested a polyclonal Antibody including Mouse α-pERK (9101, Cell signaling) in the first Antibody and Goat α-mouse 568 in the second one.

Synapsin staining

Synapsin is a useful immunohistochemical marker for the differentiation of neurospecific cells.

This phosphoprotein, which is localized on the cytoplasmic surface of synaptic vesicles, can be localized by the antibody mouse α-Syn ORF, making the neuronal cells visible under the confocal microscope. The staining occurs mainly on the outer surface of the cell membrane of neuronal cells such as glomeruli, which makes it possible to localize their exact location in the antennal lobus. (Smith, Nikulasson et al. 1993).

Confocal microscope

Imaging of fluorescently labeled thick specimen tissue is best accomplished with a confocal microscope. This is because it removes turbidity, makes finer details sharper and prevents shining through between the fluorescent dyes. In addition, one plane can be imaged after the other (Z-stack). We used the confocal laser scanning microscope (LSM 880nVIS Microscope, Carl Zeiss) for the visualization of the brains. They were put onto a slide with methyl salicylate and covered with a coverslip.

For the second Antibody with Goat α-rabbit Alexa fluor 488 and Goat α-mouse Alexa fluor 546 we used the Argon laser with the stimulation wavelength of 488nm and the Helium Neon laser (HeNe633).

For the second Antibody with Goat α-rabbit Alexa fluor 405 and Goat α-mouse Alexa fluor 633 we used the diode with the stimulation wavelength of 405nm and the Helium Neon laser (HeNe543).

For the polyclonal Antibody Goat α-mouse 568 we used the Helium Neon laser (HeNe543).

The Scans were made with 10x - 20x air lenses with the resolution of 1024 x 1024 pixel. The laser intensity was of around 70 % for Goat α-mouse 568 and Goat α-rabbit Alexa fluor 488. For Goat α-rabbit Alexa fluor 405 the laser intensity was under 10 %. All the stacks were made with an interval of 4 µm. Every Frame got scanned four times and with a speed of 5 to 6. The bandpass filter was a between 600 and 750 nm.

5. Data analysis

A total of 196 moths were double stained under various conditions. That fore the confocal laser scanning microscope (LSM 880nVIS Microscope, Carl Zeiss) was used. Among these, only 12 samples have been chosen by their visual evaluation of the quality (alignment, contamination and resolution) allowing us to analyze them in ImageJ.

Table 6: Overview of the used odors and antibodies

Odor	**1st Antibody**	**2nd Antibody**
***Cis*-3-Hexenylbenzoate**	Rabbit 9106 α-pERK (monoclonal)	Goat α -rabbit 405
		Goat α -rabbit 488
	Mouse α-Syn ORF (monoclonal)	Goat α -mouse 633

		Goat α -mouse 534
	Mouse 9101 α-pERK (polyclonal)	Goat α-mouse 568
4-Ethylguaiacol	Rabbit 9106 α-pERK (monoclonal) Mouse α-Syn ORF (monoclonal)	Goat α -rabbit 405 Goat α -mouse 633
	Mouse 9101 α-pERK (polyclonal)	Goat α-mouse 568

The main aim of this study was to identify the odor processing glomeruli in the Antennal lobe of *M. sexta*. That fore we tried out two different odors (Table 6) which were known to be perceived in very different regions of the brain (Bisch-Knaden, Dahake et al. 2018). Moreover, we tested different Antibodies, incubation times and stimulation times.

Different experimental runs were done. First the Antibodies were compared. That fore we tried 3 different ones and compared them in image quality and specific (Table 6). Further we compared the whole antennal lobes to see if Glomeruli on the stimulated scent side are getting activated. Then the different stacks got compared to each other and at least we compared all the landmark Glomeruli.
All the results were recorded through ZEN and ImageJ.

Calculating the relative brightness

The relative brightness was calculated by offsetting the 255 gray levels of the individual layers with the cell bodies on the layer. The cell bodies represented 100 % of the brightness, which ensured that stacks that were not on the same plane could be compared and that different laser intensities in the lower brain planes could be put into a relative relation.

Significance tests

The paired sample *t*-test was used for comparing in figure 9, 10 and 11, the unpaired t-test was used for figure12 and 13. The significance level was 0.05.

Results

1. Optimized resolution through Alexa fluor 405

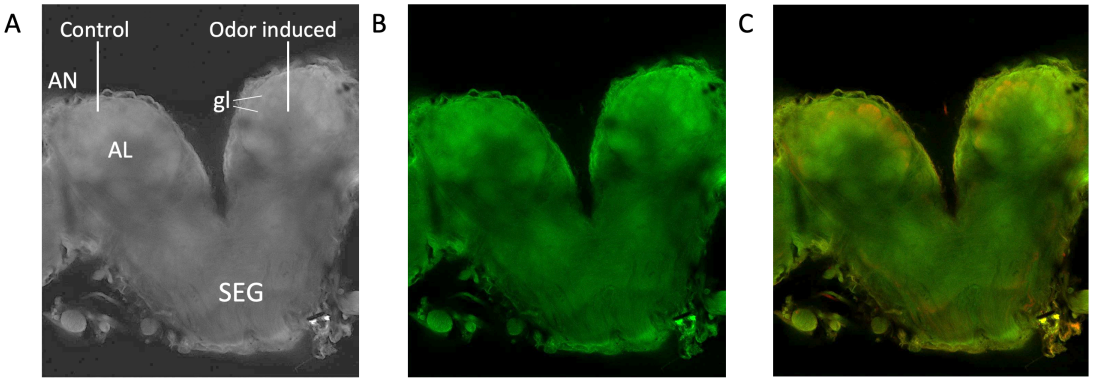

Figure 7: Double immunofluorescence staining of Manduca sexta whole brain*. Scanned with a confocal laser scanning microscope and labeled with monoclonal anti-pERK (green) antibody. (A) Brain diagram. AN, antennal nerve; AL, antennal lobes; SEG, subesophageal ganglion; gl, glomerulus (B) Alexa fluor staining of pERK (green) with the stimulation wavelength of 488 nm. (C) Alexa fluor staining of pERK with the stimulation wavelength of 488 nm and Syn ORF (red) with the stimulation wavelength of 534 nm.*

The monoclonal anti-pERK antibody specifically binds phosphorylated extracellular signal-regulated kinase (pERK). We used the monoclonal antibody with rabbit α-pERK and mouse α-syn ORF and the second antibody goat α-rabbit Alexa fluor 488 and goat α-mouse Alexa fluor 534 to identify activated glomeruli in the *M. sexta* brain. This antibody has been used in similar studies in zebrafish and in blowfly (Mirich, Illig et al. 2004, Yabuki, Koide et al. 2016, Maeda, Nisimura et al. 2020). In our experiment we induced pure HEB for 10 min and stained the brain afterwards with the previously mentioned antibody. But the image has been very blurred. Which has made it difficult to distinguish the individual antibodies (Figure 7). Also, the additional staining with the immunohistochemical marker synapsin could not help to stain the outer surface of the glomeruli to localize their exact location in the antennal lobus, because he often tied unspecified (Figure 7C). Even after expanding the incubation time of the antibodies by 2-3 days, the synapsin staining has not improved in the differentiation of individual glomeruli and stains mostly the outer glomeruli of the AL (Figure 7C). Also looking at other samples with different stimulation times (5 min, 10 min, 30 min, or pulsed stimulations with 1 s stimulation and 1 min without for 10 min), has not shown a better image quality or visible activated glomeruli. Because of that we sticked to 10 min odor exposure, which seemed to promise the best results shown in similar studies in zebrafish and some currently still unpublished papers (Yabuki, Koide et al. 2016).

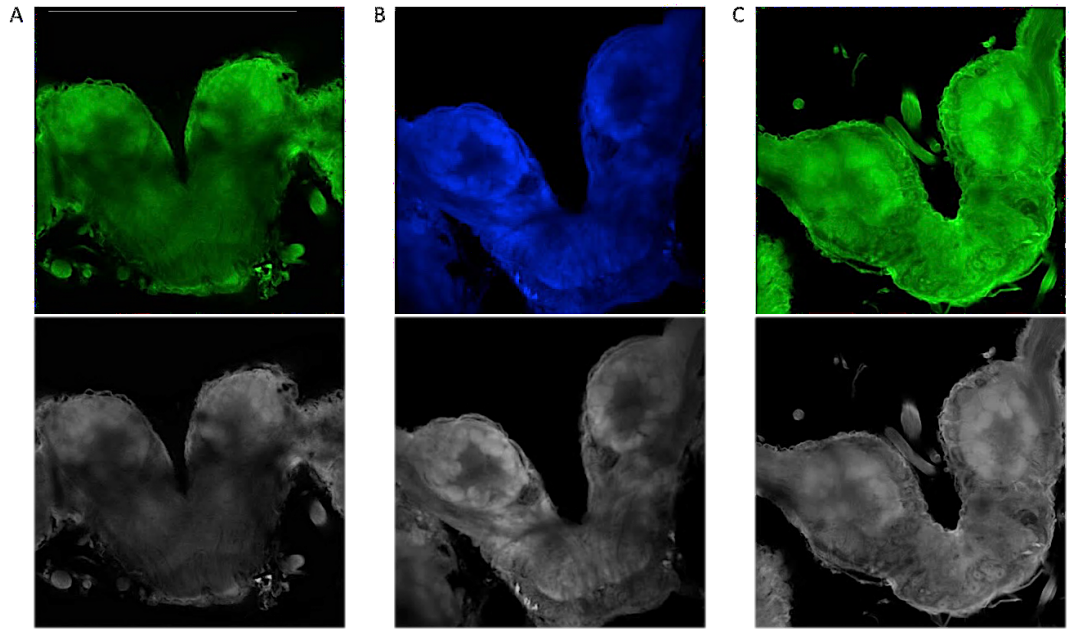

Figure 8: pERK staining with different fluorescent antibodies. All the figures were scanned with the 10x air lenses (EC Plan-Neofluar 10x/0.30 M27) and a zoom of 0.6. showing the images in color and 255 stages of grey. (A) monoclonal Goat α-rabbit Alexa fluor 488 (B) monoclonal Goat α-rabbit Alexa fluor 405 (C) polyclonal Goat α-mouse 568

When testing various second antibodies, we realized that goat α-rabbit Alexa fluor 488 monoclonal antibody (Figure 8A) did not have a clear image with clearly visible glomeruli even at a high laser power of about 70 %. This resulted in high background fluorescence. Therefore, we tested Alexa fluor with 405 nm and 633 nm to avoid overlapping spectra. The image of the goat α-rabbit Alexa fluor 405 monoclonal antibody alone produced such a clear image that it was no longer necessary to stain synapsin to identify glomeruli (Figure 8B). In addition, the laser intensity could be lowered to 2.2 % - 5.5 %, which considerably decreased background fluorescence which has been visible by lower contrast in between the brain an against the background. And was the lowest of all the tested antibodies.

Last, we tested the polyclonal antibody Mouse 9101 α-pERK with the second antibody Goat α-mouse 568, to see if it binds more specifically. However, this antibody again required very high laser intensity (70-80 %), but the image was slightly better than the monoclonal Goat α-rabbit Alexa fluor 488 which also needed high laser intensity (Figure 8C).

2. Relative brightness in different stacks is brighter under HEB

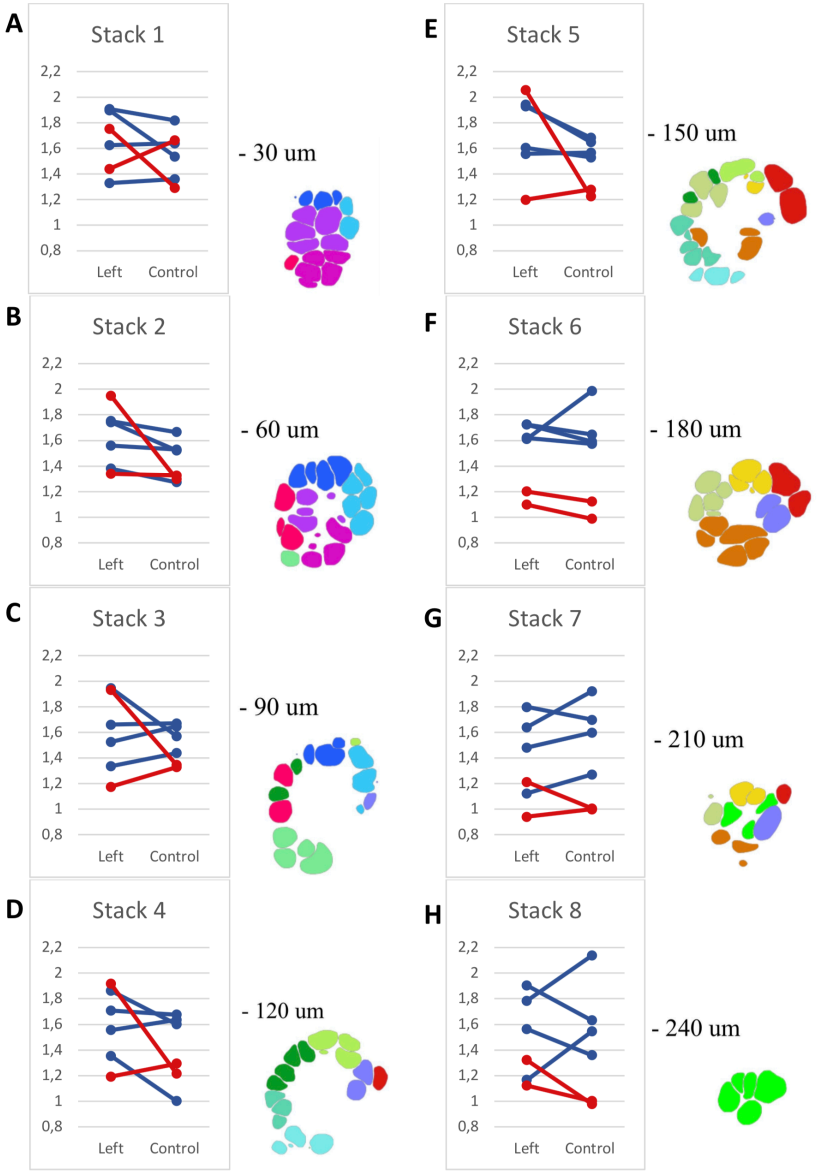

Figure 9: Brightness of eight stacks in the antennal lobe after stimulation with HEB. *Blue (red)lines depict results with the polyclonal (monoclonal) antibody. Y-axis shows relative brightness (1=brightness of cell bodies in the same stack). For every stack a paired t-test was made (A) 0,356 (B) 0,118 (C) 0,482 (D) 0,182 (E) 0,155 (F) 0,891 (G) 0,521 (H) 0,800*

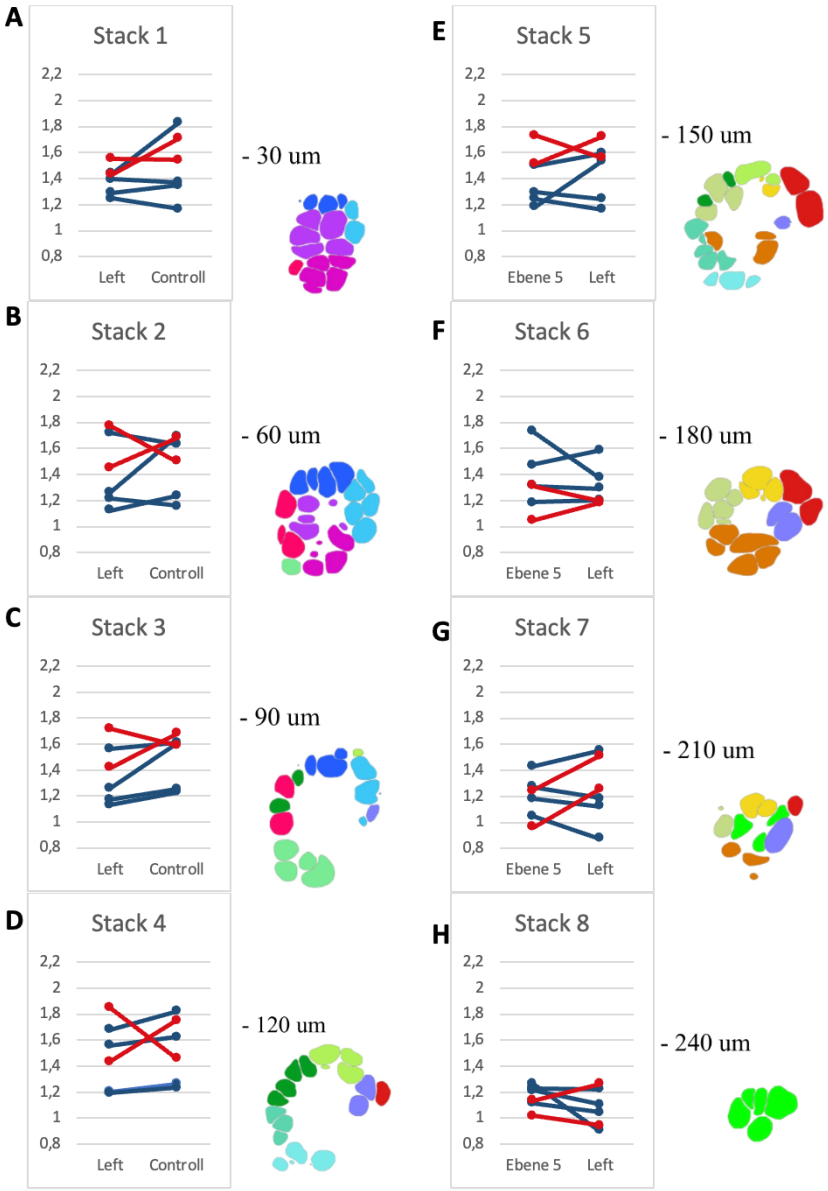

Figure 10: Brightness of eight stacks in the antennal lobe after stimulation with GUA. *Blue (red)lines depict results with the polyclonal (monoclonal) antibody. Y-axis shows relative brightness (1=brightness of cell bodies in the same stack). For every stack a paired t-test was made (A)0,239 (B) 0,604 (C) 0,144 (D) 0,690 (E) 0,517 (F) 0,627 (G) 0,484 (H) 0,267*

After stimulation with HEB, the brightness of the odor-exposed AL and the control AL did not differ significantly in any of the eight stacks examined (Figure 9). The type of antibody, monoclonal (red lines) or polyclonal (blue lines), also did not appear to have a significant effect. It was only observed that the monoclonal antibody showed a greater difference between the odor-exposed AL and the control AL. The same result as for HEB was observed when GUA was used as a stimulus (Figure 10), with slightly darker brains overall. We conclude that there is a slightly stronger with more activated glomeruli due to HEB. In addition, it is clear from this graph that the binding cannot be nonspecific because the response to the odors is different.

3. Significant differences in stack 1 and 8 through HEB

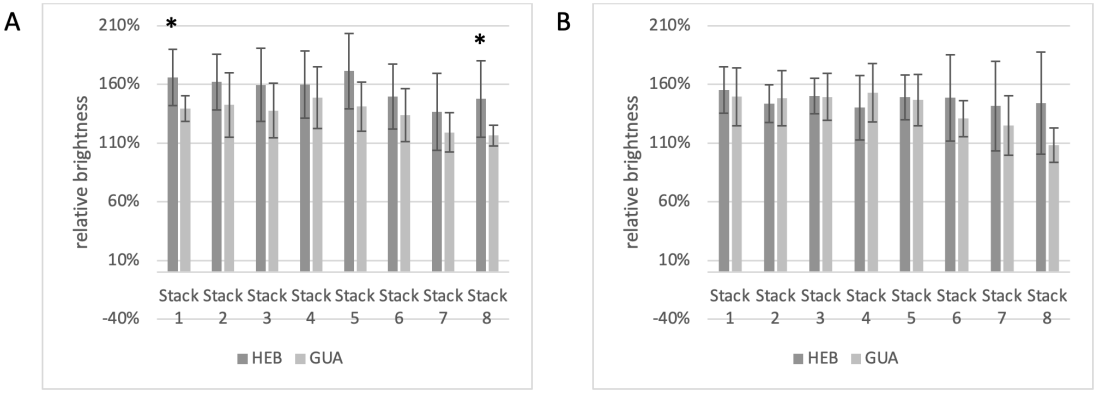

Figure 11: Comparison of the relative brightness in different stacks stimulated with HEB or GUA. *Made from 12 samples (6 stimulated with HEB and the other 6 with GUA). For each odor the monoclonal antibody got used 2 times and the polyclonal 4 times. The bars show the relative brightness with standard deviations. the significant values are marked with asterisks. (A) AL on the odor-exposed side. Homoscedastic paired t-Test for each stack: (1) 0,03 (2) 0,22 (3) 0,20 (4) 0,50 (5) 0,08 (6) 0,30 (7) 0,27 (8) 0,05 (B) Control AL. Homoscedastic paired t-Test for each stack: (1) 0,67 (2) 0,69 (3) 0,96 (4) 0,43 (5) 0,86 (6) 0,31 (7) 0,40 (8) 0,08*

First, the relative brightness of each stack was determined for each sample. Then, an average of the 6 animals per scent, represented by the bar, was calculated. The mean values of the levels of the different scents HEB and GUA were compared. Means of a paired homoscedastic t-test were used to determine whether the relative brightness differed significantly by scent at each level, and, in addition, the standard deviation was calculated from the samples.

This was only the case on the stimulated side for both stacks 1 and 8 (Figure 11).

Based on these significant differences, it can be assumed that there are glomeruli on these levels that are specifically activated by one of the odorants. In addition, it can be assumed that the cerebral hemispheres operate independently, since the control side showed no significance and the differences between odors at each level were smaller than at the stimulated side.

4. Landmark glomeruli process HEB and GUA

Furthermore, we determined the relative brightness of the 12 landmark glomeruli, which have been used for identifying the eight stacks. We determined how much brighter the single landmark glomeruli has been in comparison to the same glomeruli on the control side.

First of all, we measured the relative brightness of the landmark glomeruli of the 6 samples stimulated with HEB. Than we calculated the average and the standard deviation. Also, we did the one-sample T-test, this significance test uses the mean value of a sample to check whether the mean value of a population is equal to a given value.

The same tests were done for the second tested odor, GUA.

Landmark glomeruli DM4 and PL5 process HEB

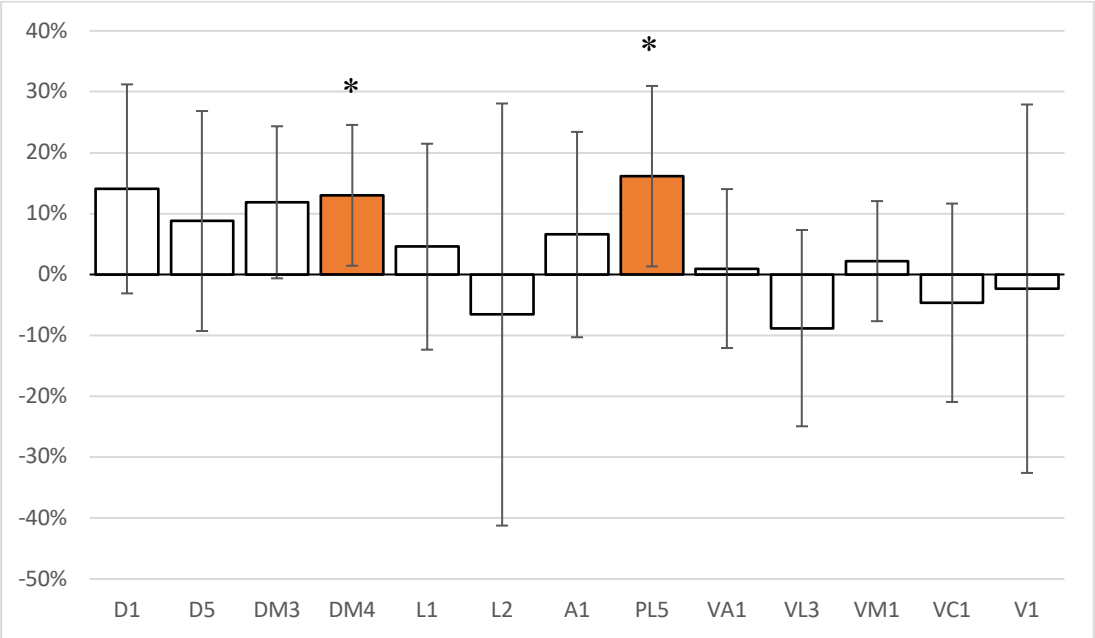

Figure 12: With HEB stimulated landmark glomeruli percentage difference in relative brightness against the respective landmark glomeruli on the control. *One sample T-test on the 6 samples (D1) 0,10 (D5) 0.29 (DM3) 0,07 (DM4) 0,04 (L1) 0,54 (L2) 0,66 (A1) 0,38 (PL5) 0,04 (VA1) 0,86 (VL3) 0,24 (VM1) 0,61 (VC1) 0,52 (V1) 0,86*

Stimulation with HEB led to the activation of two of the 13 analyzed landmark glomeruli, as they were on average 13% (DM4) and 16% (PL5) brighter than the corresponding glomeruli on the control side (Figure 12).

Landmark glomeruli VL3 and V1 process GUA

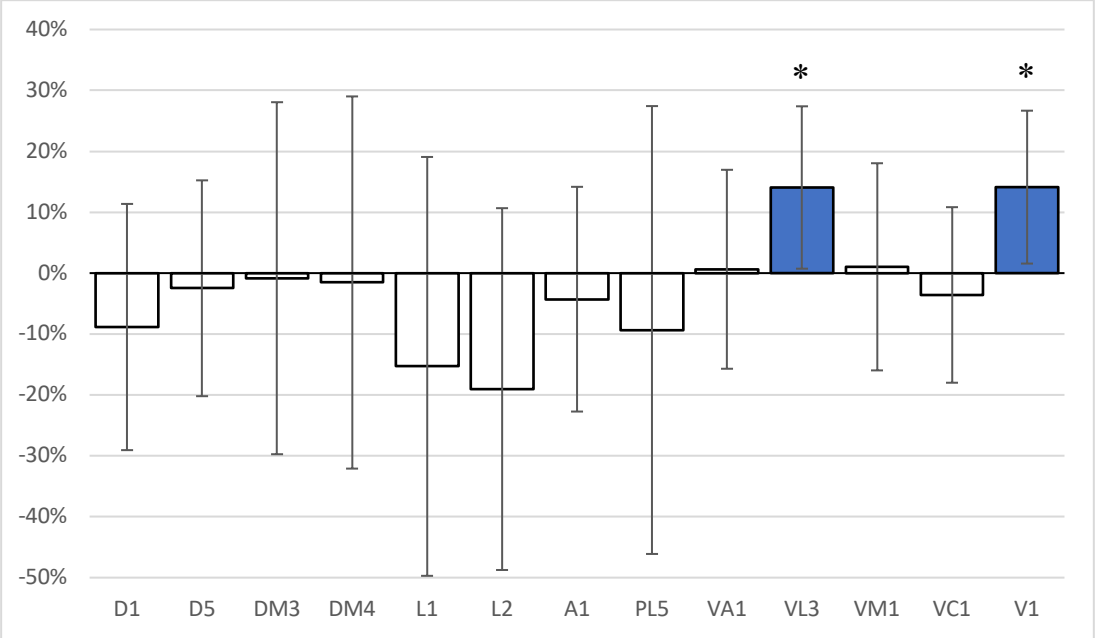

Figure 13: With GUA stimulated landmark glomeruli percentage difference in relative brightness against the respective landmark glomeruli on the control. *One sample t-test on the 6 samples (D1) 0,33 (D5) 0.74 (DM3) 0,95 (DM4) 0,91 (L1) 0,33 (L2) 0,18 (A1) 0,59 (PL5) 0,56 (VA1) 0,93 (VL3) 0,05 (VM1) 0,89 (VC1) 0,57 (V1) 0,04*

Also, stimulation with GUA activated two of the landmark glomeruli (VL3 and V1) that were on average 14% brighter on the odor-exposed side than on the control side (Figure 13).

Stimulation of HEB and GUA activates two glomeruli each, which are relatively far away from each other and are not the same.

Discussion

In this study, we tried to establish an immunohistochemical method to trace odor-induced neural activity in the AL of *M. sexta*.

To identify the activation of the glomeruli we detected the phosphorylated ERK by second antibody-staining. We compared three antibodies, of which 2 were monoclonal and 1 polyclonal. We found that the monoclonal antibody rabbit 9106 α-pERK visualist through goat α-rabbit Alexa fluor 405 monoclonal antibody was the most responsive, which could lead to the fact, that the monospecificity of the monoclonal antibody is useful for assessing changes in phosphorylation state of ERK, and to identify individual members of protein families such as the membrane protein synapsin. However, it cannot be ruled out that the polyclonal antibody, although having poorer resolution, binds more specifically to the reaction product pERK, since the antibodies are each formed against a specific epitope (Lipman, Jackson et al. 2005).

For the choice of the second fluorescent antibody, we decided to use goat α-rabbit Alexa fluor 405 and goat α-mouse 633 instead of α-rabbit Alexa fluor 488 and goat α-mouse 534 because the wavelengths were not overlapping what reduces false colabeling results.

Overall, the synapsin staining that should help to identify the glomeruli under the confocal microscope was not as successful as expected. The staining might be improved by a longer incubation time. However, it was no longer necessary due to the good resolution achieved with goat α-rabbit Alexa fluor 405, which in addition saved time during scanning.

Despite the already changed incubation times, further experiments should be considered to also improve the synapsin staining for further experiments. For this purpose, the concentration of syn ORF in the second antibody should be increased. It is also questionable whether the first antibodies used are suitable for *Manduca sexta* and bind specifically enough, as they also seemed to bind to the control brain hemispheres.

Further, we looked at the relative brightness of the stimulated and the control AL. It turned out that the scent-exposed side is not significantly brighter, when we analyzed eight representative stacks of each AL. Which in turn makes it difficult to see under the confocal microscope whether the stimulation has worked or not.

This should actually not be the case, since the antibodies should specifically bind only the resulting pERK, and all olfactory sensory neurons project into the ipsilateral antennal lobe, so the signal should not be seen on the control AL (Homberg, Montague et al. 1988, Christensen, Harrow et al. 1995). Based on the results obtained, it is of course possible that the antibody binds and recognizes pERK, but not specifically enough. And thus, the staining is also present in the surrounding tissue. The fact that it can still be useful to detect pERK is then again only shown in the exact analysis and the direct comparison.
For this reason, it should be checked in further experiments whether the second antibody does not simply bind non-specifically. For this purpose, the experiment would have to be performed as described in the methods without the first antibody, and then there should be no imaging under the confocal microscope. It would also be useful to perform the experiment without scent, or to stimulate both antenna of an animal to exclude transmission between the antennal lobes which has been done in in similar experiments (Maeda, Nisimura et al. 2020). Then of course the direct negative control would be missing.

In addition, the results showed that *cis*-3-hexenyl benzoate and 4-Ethylguaiacol elicited a different response in the antennal lobe of *M. sexta*. The response to HEB was significantly greater than to GUA in both the left and right AL. This stronger stimulation by HEB, might be related to the fact that more glomeruli are activated.
Although the stimulated side was not always brighter as expected, there was a clearly visible difference in responses when odorants were compared, which allowed us to locate two levels with a significant difference. It can be assumed that the signal-processing glomeruli stimulated by the odorant are located at these two levels.

Additionally, HEB and GUA activated 2 glomeruli each that are located in different regions of the antennal lobe as we expected based on results from calcium imaging experiments (Bisch-Knaden, Dahake et al. 2018). Since the approximate location of calcium imaging corresponds to that of the antibodies localized by pERK, it can be assumed that pERK can be used as a marker for odor-induced activity in the brain of *M. sexta*.
Of the localized glomeruli, only one was on one of the significantly brighter stacks. All other three glomeruli were on stacks that were not significantly brighter. This means that there must be some unanalyzed activated glomeruli on the brighter stacks.

It is also possible that there are other unseen activated glomeruli on the non-significant stacks. These could still be unseen due to other darker glomeruli on their stack.
Overall, significant brightness can help us find activated glomeruli, but it does not reduce the radius in which we need to search.

Overall, the determination of the stimulated glomeruli proved to be very difficult because the identification of the 12 landmark glomeruli was very time consuming and was only the beginning of the multistep analysis. The best option, of course, would be to assess all 70 glomeruli. However, the position, size and shape of glomeruli may change due to fixations, further complicating localization (Grabe et al. 2016) (Grosse-Wilde, Kuebler et al. 2011). In addition, usually not only one glomerulus but several are stimulated which makes differentiation difficult due to the lower contrast between them (Malnic, Hirono et al. 1999). It would then be imperative to achieve very good resolution and further optimize synaptic staining.
Also, due to the different spatial arrangement of the antennal lobes, different brightness may occur, which we tried to compensate by the normalization method we applied. Nevertheless, in future experiments we should work with a uniform laser intensity to compare the levels even better without the need to normalize the results.

The main goal of establishing an immunohistochemical method to detect odor-induced neural activity in the AL of *M. sexta* was achieved in the end. Although not as originally expected. Identification of all glomeruli involved in the recognition of two odors was not possible using immunostaining with pERK. This was partly because it was not foreseeable that the scans would yield results that could only be seen in the analysis. In fact, this was not the case in previous studies (Yabuki, Koide et al. 2016, Maeda, Nisimura et al. 2020), and may be because the antibody is not specific enough. Nevertheless, success was achieved in identifying the landmark glomeruli involved, confirming that pERK may be suitable for localizing glomeruli activated by odorants. If the method could be further developed, it would be a great advantage over the calcium image since an exact spatial determination would also be possible in the 3D model and higher processing regions could also be investigated.

In further experiments, the method should therefore be improved, and consideration should be given to repeating the same experiments and obtaining more samples, e.g., also in HEB, to determine whether further landmark glomeruli are activated. Also, a lower scent concentration could be tested to activate only one glomerulus at a time.

References

Biotechnology GUA, N. C. f. (2021). 4-Ethyl-2-methoxyphenol. https://pubchem.ncbi.nlm.nih.gov/compound/4-Ethyl-2-methoxyphenol, PubChem.

Biotechnology HEB, N. C. f. (2021). cis-3-Hexenyl benzoate. https://pubchem.ncbi.nlm.nih.gov/compound/cis-3-Hexenyl-benzoate., PubChem.

Bisch-Knaden, S., A. Dahake, S. Sachse, M. Knaden and B. S. Hansson (2018). "Spatial Representation of Feeding and Oviposition Odors in the Brain of a Hawkmoth." Cell Reports **22**(9): 2482-2492.

Christensen, T. A., I. D. Harrow, C. Cuzzocrea, P. W. Randolph and J. G. Hildebrand (1995). "Distinct projections of two populations of olfactory receptor axons in the antennal lobe of the sphinx moth Manduca sexta." Chemical senses **20**(3): 313-323.

Couto, A., M. Alenius and B. J. Dickson (2005). "Molecular, anatomical, and functional organization of the Drosophila olfactory system." Current Biology **15**(17): 1535-1547.

Couty, A., H. Van Emden, J. N. Perry, J. Hardie, J. A. Pickett and L. J. Wadhams (2006). "The roles of olfaction and vision in host-plant finding by the diamondback moth, Plutella xylostella." Physiological Entomology **31**(2): 134-145.

Galizia, C. G. and W. Rössler (2010). "Parallel olfactory systems in insects: anatomy and function." Annual review of entomology **55**: 399-420.

Grabe, V., A. Baschwitz, H. K. Dweck, S. Lavista-Llanos, B. S. Hansson and S. Sachse (2016). "Elucidating the neuronal architecture of olfactory glomeruli in the Drosophila antennal lobe." Cell reports **16**(12): 3401-3413.

Grosse-Wilde, E., L. S. Kuebler, S. Bucks, H. Vogel, D. Wicher and B. S. Hansson (2011). "Antennal transcriptome of Manduca sexta." Proceedings of the National Academy of Sciences **108**(18): 7449-7454.

Hansson, B. (1995). "Olfaction in lepidoptera." Experientia **51**(11): 1003-1027.
Hansson, B. S. and M. C. Stensmyr (2011). "Evolution of insect olfaction." Neuron **72**(5): 698-711.

Hildebrand, J. G. (1995). "Analysis of chemical signals by nervous systems." Proceedings of the National Academy of Sciences **92**(1): 67-74.

Hildebrand, J. G. and G. M. Shepherd (1997). "Mechanisms of olfactory discrimination: converging evidence for common principles across phyla." Annual review of neuroscience **20**(1): 595-631.

Homberg, U., R. Montague and J. G. Hildebrand (1988). "Anatomy of antenno-cerebral pathways in the brain of the sphinx moth Manduca sexta." Cell and tissue research **254**(2): 255-281.

Kanost, M. R., E. L. Arrese, X. Cao, Y.-R. Chen, S. Chellapilla, M. R. Goldsmith, E. Grosse-Wilde, D. G. Heckel, N. Herndon and H. Jiang (2016). "Multifaceted biological insights from a draft genome sequence of the tobacco hornworm moth, Manduca sexta." Insect biochemistry and molecular biology **76**: 118-147.

King, J. R., T. A. Christensen and J. G. Hildebrand (2000). "Response characteristics of an identified, sexually dimorphic olfactory glomerulus." Journal of Neuroscience **20**(6): 2391-2399.

Lipman, N. S., L. R. Jackson, L. J. Trudel and F. Weis-Garcia (2005). "Monoclonal versus polyclonal antibodies: distinguishing characteristics, applications, and information resources." ILAR journal **46**(3): 258-268.

Ma, B.-W., X.-C. Zhao, B. G. Berg, G.-Y. Xie, Q.-B. Tang and G.-R. Wang (2017). "Central Projections of Antennal and Labial Palp Sensory Neurons in the Migratory Armyworm Mythimna separata." Frontiers in Cellular Neuroscience **11**(370).

Maeda, T., T. Nisimura, S. Habe, T. Uebi and M. Ozaki (2020). "Visualization of antennal lobe glomeruli activated by nonappetitive D-limonene and appetitive 1-octen-3-ol odors via two types of olfactory organs in the blowfly Phormia regina." Zoological Letters **6**(1): 1-13.
Malnic, B., J. Hirono, T. Sato and L. B. Buck (1999). "Combinatorial receptor codes for odors." Cell **96**(5): 713-723.

Mirich, J. M., K. R. Illig and P. C. Brunjes (2004). "Experience-dependent activation of extracellular signal-related kinase (ERK) in the olfactory bulb." Journal of comparative Neurology **479**(2): 234-241.

Mitaka, Y., K. Kobayashi, A. Mikheyev, M. M. Tin, Y. Watanabe and K. Matsuura (2016). "Caste-specific and sex-specific expression of chemoreceptor genes in a termite." PLoS One **11**(1): e0146125.

Miyashita, T., E. Kikuchi, J. Horiuchi and M. Saitoe (2018). "Long-term memory engram cells are established by c-Fos/CREB transcriptional cycling." Cell Reports **25**(10): 2716-2728. e2713.

Reisenman, C. and J. Riffell (2015). "The neural bases of host plant selection in a Neuroecology framework." Frontiers in Physiology **6**(229).

Riffell, J. A., H. Lei and J. G. Hildebrand (2009). "Neural correlates of behavior in the moth Manduca sexta in response to complex odors." Proceedings of the National Academy of Sciences **106**(46): 19219-19226.

Riffell, J. A., E. Shlizerman, E. Sanders, L. Abrell, B. Medina, A. J. Hinterwirth and J. N. Kutz (2014). "Flower discrimination by pollinators in a dynamic chemical environment." Science **344**(6191): 1515-1518.

Rountree, D. B. and W. E. Bollenbacher (1986). "The release of the prothoracicotropic hormone in the tobacco hornworm, Manduca sexta, is controlled intrinsically by juvenile hormone." Journal of Experimental Biology **120**(1): 41-58.

Shields, V. and J. G. Hildebrand (1999). "Fine structure of antennal sensilla of the female sphinx moth, Manduca sexta (Lepidoptera: Sphingidae). II. Auriculate, coeloconic, and styliform complex sensilla." Canadian journal of zoology **77**(2): 302-313.

Shields, V. D. C. and J. G. Hildebrand (2001). "Responses of a population of antennal olfactory receptor cells in the female moth Manduca sexta to plant-associated volatile organic compounds." Journal of Comparative Physiology A **186**(12): 1135-1151.

Smith, T., S. Nikulasson, U. De Girolami and L. De Gennaro (1993). "Immunohistochemistry of synapsin I and synaptophysin in human nervous system and neuroendocrine tumors. Applications in diagnostic neuro-oncology." Clinical neuropathology **12**(6): 335-342.

Tumlinson, J. H., M. M. Brennan, R. E. Doolittle, E. R. Mitchell, A. Brabham, B. E. Mazomenos, A. H. Baumhover and D. M. Jackson (1989). "Identification of a pheromone blend attractive to Manduca sexta (L.) males in a wind tunnel." Archives of Insect Biochemistry and Physiology **10**(4): 255-271.

Vosshall, L. B., A. M. Wong and R. Axel (2000). "An olfactory sensory map in the fly brain." Cell **102**(2): 147-159.

Yabuki, Y., T. Koide, N. Miyasaka, N. Wakisaka, M. Masuda, M. Ohkura, J. Nakai, K. Tsuge, S. Tsuchiya and Y. Sugimoto (2016). "Olfactory receptor for prostaglandin F 2α mediates male fish courtship behavior." Nature neuroscience **19**(7): 897-904.

Acknowledgement

First and foremost, I would like to thank Bill Hanson, the group leader of the Evolutionary Neuroethology Department, and Sonja Bisch-Knaden for the opportunity to write my bachelor's thesis in their Institute.
Sonja was the best help I could have imagined and was not only always available and helpful, but also did more for me than she had to.
I would also like to thank Nicole van Dam for supervising this work.
I owe special thanks to my mentor, Yusuke, who introduced me to all the experiments and always had advice or a solution ready when times got tough.
I would also like to thank the entire department for the nice conversations. A special thanks goes to Sascha, who always had an open ear for me and to Roland, who made my tweezers look like new again. Also, to Veit who supported me very well at the confocal microscope.

Last but not least, I would like to thank my friends and roommates for the great support and the 3 wonderful years during my bachelor studies.

Declaration of Independent Assignment

I hereby declare that I have written this thesis independently and that I have not used any auxiliary materials other than those indicated. All passages that are taken verbatim or in spirit from other works, including illustrations, are marked with references.

The thesis has not been previously submitted whether to the Friedrich-Schiller-University, Jena or to any other university.

Jena, 29.09.2021 …….
Luka Hecht